PERGAMON

Deep-Sea Research II 48 (2001) 159–178

DEEP-SEA RESEARCH
PART II

www.elsevier.com/locate/dsr2

Influence of a Gulf Stream warm-core ring on water mass and chlorophyll distributions along the southern flank of Georges Bank☆

J.P. Ryan[a,*,1], J.A. Yoder[a], D.W. Townsend[b]

[a]*Graduate School of Oceanography, University of Rhode Island, Narragansett, RI 02882, USA*
[b]*School of Marine Sciences, University of Maine, Orono, Maine 04469, USA*

Received 12 August 1998; received in revised form 16 September 1999; accepted 10 December 1999

Abstract

During late spring 1997, a Gulf Stream warm-core ring (WCR) strongly influenced water mass and chlorophyll distributions along the southern flank of Georges Bank. Entrainment of Georges Bank shelf water by the WCR, centered at the central southern flank, persisted through May. By late May, shelf water encircled nearly the entire WCR, and horizontal convergence toward the central southern flank was evident. Scotian Shelf water (SSW) extended across Northeast Channel, onto Georges Bank near the northeast peak, and along the southern flank between the 60-m isobath and the shelfbreak front. SSW extended furthest southwest along the southern flank shelfbreak. Satellite imagery from the ocean color and temperature sensor (OCTS) showed that by late May, in addition to the high chlorophyll concentrations within the entrained shelf water encircling the WCR, pigment rich bands of chlorophyll developed along the 60- and 100-m isobaths. Where this biological enhancement developed along > 100 km of the shelfbreak (100-m isobath), shelf waters extended furthest seaward due to entrainment by the WCR. The enhanced shelfbreak chlorophyll was sampled in situ along two transects separated by ≈ 40 km along shelf. Along both transects, the enhanced chlorophyll coincided with divergent cross-shelf flow, maximum along-shelf flow and minimum surface temperature. Coincidence of the highest surface chlorophyll and lowest surface temperature with divergent cross-shelf flow is consistent with upwelling. Coincidence with along-shelf jets and their associated vertical shear is consistent with turbulent vertical mixing. The importance of turbulent vertical mixing was supported. Maximum velocity at the shelfbreak coincided with the subsurface temperature minimum of SSW near 30-m depth. Estimated gradient Richardson numbers (Ri) above the SSW were below critical (< 0.25) within the shelfbreak chlorophyll maximum along both transects, and surface chlorophyll was significantly, inversely correlated with Ri along the southern flank. WCR entrainment of shelf water continued into June as

☆ Paper published in December 2000.

* Corresponding author. Tel.: 1-831-775-1978, fax: 1-831-775-1652.
E-mail address: ryjo@mbari.org (J.P. Ryan).
[1] Now at MBARI, 7700 Sandholdt Road, Moss Landing, CA 95039-0628, USA.

0967-0645/01/$ - see front matter
PII: S0967-0645(00)00117-X

the WCR propagated southwestward. On June 11, high chlorophyll concentrations along the shelfbreak north of the WCR were observed by the OCTS. Satellite sea-surface temperature showed that in addition to WCR entrainment, breaking waves ($\lambda \approx 30$ km) of the shelf-slope front coincided directly with the locally enhanced chlorophyll. The waves propagated west at ≈ 12 km day^{-1}. Vertical mixing due to these breaking frontal waves may have contributed to local nutrient enrichment of near-surface waters at the shelfbreak. © 2000 Published by Elsevier Science Ltd.

1. Introduction

Gulf Stream warm-core rings (WCRs) are anticyclonic eddies that form when steep northward meanders close upon themselves and detach from the stream (Saunders, 1971). Approximately 2 km in depth and 60–200 km in width, WCRs rotate with maximum speeds of ≈ 2 m s^{-1} near the surface as they translate southwestward through the Slope Sea (Fig. 1) at an average speed of ≈ 6 cm s^{-1} (Haliwell and Mooers, 1979; Richardson, 1983; Joyce, 1984; Brown et al., 1986). Initially, WCRs comprise primarily two water masses: a core of Sargasso Sea water and circumfluent Gulf Stream water. As they age, they mix with the surrounding water masses and decrease in diameter (Brown et al., 1986). All are ultimately absorbed by the Gulf Stream. During their lifetimes, which can exceed a year, WCRs can influence the distributions of many water masses off northeastern North America (Fig. 1): waters of the Mid-Atlantic Bight (MAB) shelf, Georges Bank, Gulf of Maine, Scotian Shelf, Slope Sea, Gulf Stream, and Sargasso Sea (e.g. Evans et al., 1985; Garfield and Evans, 1987; Churchill et al., 1986; 1993).

When WCRs impact the front between continental shelf and slope waters, they can entrain shelf water into the Slope Sea. Entrainment generally initiates near the northeast periphery of the WCR, often in association with small-scale cyclone development (Evans et al., 1985; Kennelly et al., 1985; Ramp, 1986). Between Cape Cod and Cape Sable (Fig. 1), WCR entrainment of shelf water is observed approximately 70% of the time in satellite sea-surface temperature (SST) imagery and has been estimated conservatively at 5700 km^3 yr^{-1} (Garfield and Evans, 1987). Based on synoptic survey of shelf water filaments entrained by WCRs, Schlitz (1999) estimated volumes ranging between 58 and 290 km^3. More WCRs interact with shelf water along the southern flank of Georges Bank than along the MAB shelf, and entrainment is highly variable interannually (Haliwell and Mooers, 1979; Garfield and Evans, 1987). In some years, offshore transport by WCR entrainment could equal more than half of the along-shelf transport on Georges Bank (Flagg, 1987). In other years, WCR entrainment from Georges Bank may be entirely absent.

Because offshore transport of shelf water can influence larval recruitment and carbon flux, the source region of shelf water entrained by WCRs is an important consideration. Due to the retrograde slope of the shelfbreak front, approximately half of the shelf water mass lies seaward of the shelfbreak, above the front (Wright, 1976; Wright and Parker, 1976). Analyses of WCR entrainment occurrences have shown the source region of shelf water filaments to be seaward of the shelfbreak (Ramp, 1986; Schlitz, 1999). More specifically, entrained waters were apparently from a narrow band along the shelf water side of the front. Ramp (1986) found that the source region can extend along shelf ahead of the WCR center, or as much as 1 ring diameter behind the WCR trailing flank.

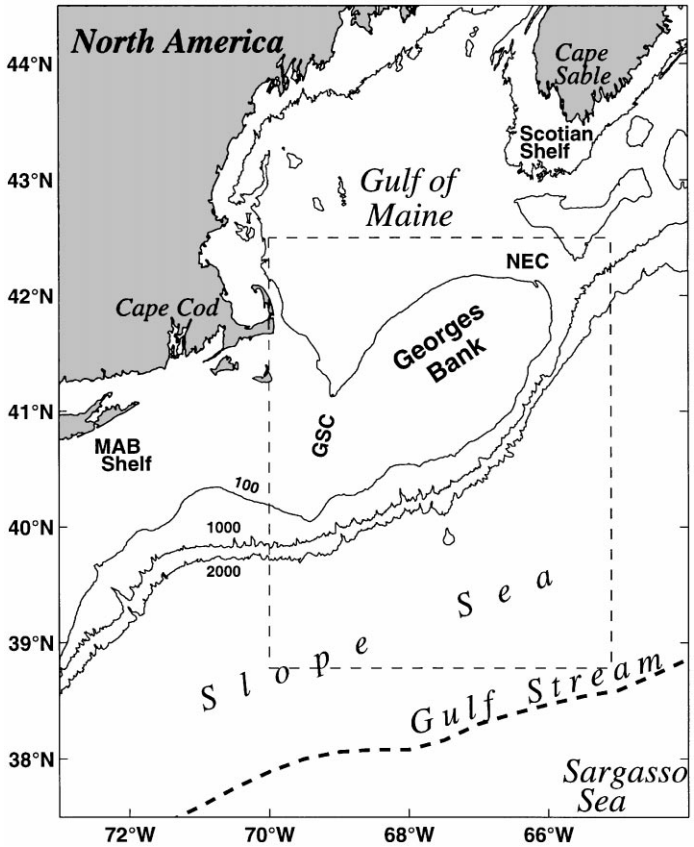

Fig. 1. Map of the study region. Reference points used in the text are labeled; GSC is Great South Channel; NEC is Northeast Channel. The 100-m isobath defines the approximate location of the shelfbreak and the outline of Georges Bank. The mean position of the Gulf Stream north wall, defined from 12 yr of satellite sea-surface temperature (SST) imagery (Gilman, 1988), is shown as the thick dashed line. The dashed box marks the domain of the SST maps shown in Fig. 2.

WCRs influence not only water mass distributions, but also phytoplankton distributions and processes. Interaction of WCRs with the surrounding hydrography can enhance phytoplankton biomass within the core and along the ring periphery (Smith and Baker, 1985; Yentsch and Phinney, 1985; Nelson et al., 1989). Advection of pigment-rich water from the shelf by WCRs is a principal cause of variability in satellite-observed chlorophyll in and around WCRs (Garcia-Moliner and Yoder, 1994; Ryan et al., 1999a). In addition to filaments of chlorophyll rich shelf water drawn offshore by WCR circulation, pigment-enhanced filaments can develop along the shelfbreak in coincidence with WCR entrainment. Evident annually during late spring to early summer is an association between seaward entrainment of shelf water, by WCRs or other frontal disturbances, and enhanced chlorophyll along the shelfbreak of the MAB and Georges Bank (Ryan et al., 1999a).

During late spring of 1997, two occurrences of enhanced chlorophyll along the northeast US continental shelfbreak were observed by the ocean color and temperature sensor (OCTS) satellite

instrument. The first developed during early May along >200 km of the MAB shelfbreak. Its dynamical basis was upwelling of shelf water along isopycnals in the shelfbreak front during seaward entrainment by frontal meanders (Ryan et al., 1999b). The second occurrence developed along >100 km of the southern flank of Georges Bank in association with seaward entrainment of shelf water by a WCR and intrusion of Scotian Shelf water along the southern flank. Our purposes here are to examine hydrographic and biological structure of this occurrence, and to define a dynamical basis for the enhanced shelfbreak chlorophyll.

2. Methods

2.1. Satellite-derived observations

OCTS imagery and ancillary data required for its processing were acquired from NASA Goddard Space Flight Center. Ancillary data were daily ozone maps from the total ozone mapping spectrometer, and meteorological variables from the National Centers for Environmental Prediction (McClain et al., 1994). A single-scattering algorithm was used for atmospheric correction (Gordon et al., 1983), and a 3-band chlorophyll algorithm (Saitoh et al., 1997) was used for calculating chlorophyll *a* (hereafter OCTS-Chl). SST imagery from the advanced very high resolution radiometer (AVHRR) was acquired from the Graduate School of Oceanography, University of Rhode Island. OCTS and AVHRR imagery were mapped to the same projection.

2.2. In situ observations

During the late May period of strong WCR entrainment, Georges Bank was sampled in situ during a US Global Ocean Ecosystems Dynamics (GLOBEC) survey conducted on the RV *Albatross IV* (Mountain et al., 1997). This survey included CTD casts, nutrient and chlorophyll measurements at CTD stations, and continuous underway temperature, salinity, and fluorescence measurements (hull thermistor at ≈ 5 m; water pumped from ≈ 2.5 m for salinity and fluorescence measurements). At GLOBEC standard stations, profiles were from a calibrated *Neil Brown Mark V* CTD equipped with a fluorometer; the fluorometer was calibrated with extractive chlorophyll measurements. At all other stations, CTD profiles were from the upcast of a calibrated Seabird CTD attached to a plankton net; the oblique plankton tows typically covered ≈ 1 km during a combined down-up cast (Mountain et al., 1997). Thermosalinograph salinity was calibrated by comparison with CTD salinity (calibrated with bottle samples). Calibration of the underway fluorometer was by linear regression of the shallowest chlorophyll measurements (2–5 m) and mean fluorometer voltage calculated as inverse-distance weighted means of observations within a 2-km radius of each station.

During the GLOBEC survey, water velocity was measured using a 300-kHz RDI broadband acoustic doppler current profiler (ADCP). The ADCP was configured to record 1-m depth bins, with the shallowest bin at 8 m, and ≈ 20 min ensembles. Water velocities were averaged into 30 min bins, corresponding to a distance of ≈ 5 km when the ship was underway. To examine the enhanced chlorophyll along the shelfbreak relative to the potential for turbulent vertical mixing, we

used total velocity and CTD profiles to compute gradient Richardson numbers (Ri). Ri defines the relative importance of the stabilizing influence of vertical density stratification versus the destabilizing influence of vertical shear in horizontal velocity:

$$\mathrm{Ri} = \frac{-g/\rho_0(\partial\rho/\partial z)}{(\partial u/\partial z)^2 + (\partial v/\partial z)^2} \quad (1)$$

where g is gravitational acceleration, and ρ_0 is the average density in the layer. It is generally accepted that flows become turbulent below $\mathrm{Ri} = 0.25$ (Pond and Pickard, 1983). Density was calculated from temperature, salinity, and pressure using MATLAB code from the CSIRO Oceanographic Toolbox (Morgan, 1992). This code uses the UNESCO 1983 polynomial (Fofonoff and Millard, 1983). Total velocity observations from the ADCP bin temporally nearest each CTD cast were used. Ri was calculated at the midpoint of every velocity depth bin, and median Ri above 20 m was used to represent potential for turbulent vertical mixing in the upper water column. The depth of 20 m was chosen because a subsurface chlorophyll maximum was repeatedly observed between ≈ 10 and 20 m during the survey. A subsurface chlorophyll maximum develops in the thermocline of shelf waters following the spring bloom, when near-surface nutrients are depleted and nutrient supply from below the thermocline is required for phytoplankton growth. Thus mixing above the subsurface chlorophyll maximum could introduce both nutrients and chlorophyll to near-surface waters. Surface fluorometric chlorophyll from underway measurement was used for correlation with Ri because CTD fluorescence measurements were too sparse (the *Mark V* CTD with fluorometer was used only at a subset of the stations). Station surface fluorometric chlorophyll values were calculated as inverse-distance weighted means of observations within a 2-km radius of each station. Because both variables were approximately log-normally distributed, correlation was computed from log-transformed values. Significance was tested via t-test.

Tidal flows are very strong and complex over Georges Bank (Moody et al., 1984; Brown and Moody, 1987). Thus examination of sub-tidal flow from underway ADCP observations is both important and difficult. To estimate and remove the principal tidal constituents (M_2, S_2, N_2, K_1 and M_1), we used the methodology developed by Candela et al. (1992), as optimized for Georges Bank by C. Flagg and Y. Shi (Brookhaven National Laboratory). Observations in the multi-year velocity database required for tidal analysis did not extend to the western and eastern extremities of the southern flank, so calculation of subtidal flow was limited to the central southern flank.

3. Results

Our ability to combine satellite and in situ observations was limited to the period of the May GLOBEC survey. Therefore, most of the results focus on structure and processes along the southern flank during May of 1997. In Section 3.1, we illustrate WCR influence on water mass distributions and circulation. In Section 3.2, we present pigment field structure related to the WCR entrainment and associated water mass distributions. In Section 3.3, we examine processes associated with the enhanced chlorophyll along the southern flank.

3.1. WCR influence on water mass distributions

Satellite SST during late May 1997 defined widespread influence of the WCR on water mass distributions on and around Georges Bank (Fig. 2). In the contour plots of SST, the approximate surface expression of Scotian Shelf water (SSW) influence is represented by dashed isotherms. This is termed influence because SSW mixed with adjacent waters. As will be shown, the low-salinity signature of SSW was observed in situ over northeastern Georges Bank and along the southern flank shelfbreak, and its low-temperature signature was observed subsurface between the 60-m isobath and the shelfbreak front. For May 12 and 18 (Fig. 2a, b), the 7°C isotherm is used to delineate SSW influence. Regional SST was significantly warmer by May 28 (Fig. 2c), and a warmer

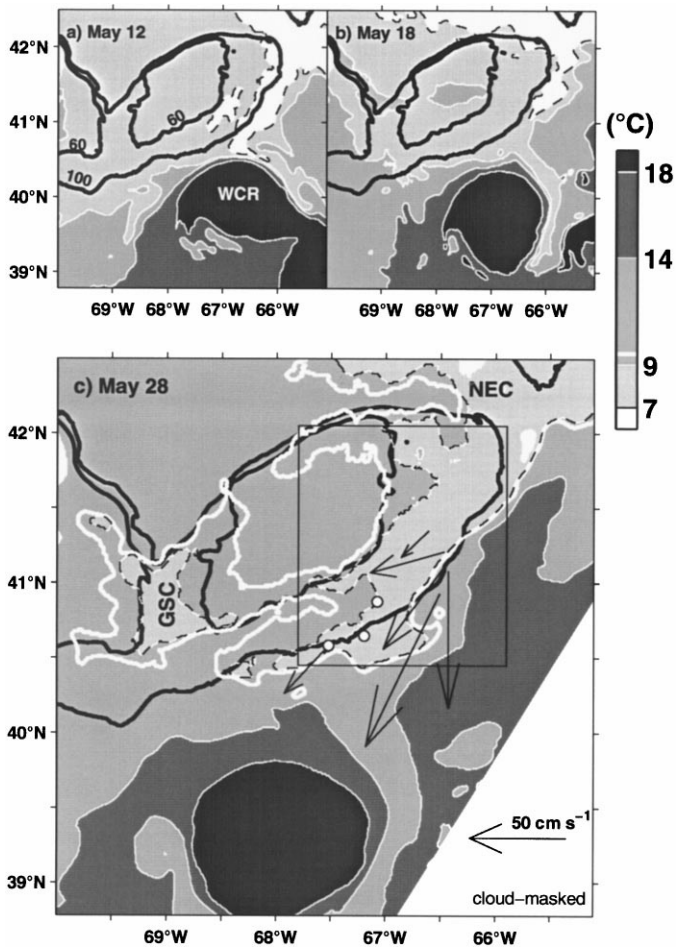

Fig. 2. SST distributions from AVHRR imagery during May of 1997. In (c), the box delineates the domain of subsurface temperature shown in Fig. 3, and the three circles in the southwest quadrant of this box define the locations of CTD profiles shown in Fig. 4. Vectors show average subtidal velocity within the layer 14–26 m during a survey of the southern flank, May 23–24.

(9°C) isotherm is used to delineate SSW influence (excluding GSC). The sequence described below using the contour plots is clearly defined in an animation of SST (online, *http://brando.gso.uri.edu/SST*).

By early April, the WCR was south of the central southern flank of Georges Bank. It remained ≈ 100 km south of the shelfbreak through April. During early May, interaction with a northward meander of the Gulf Stream forced the WCR toward the central southern flank of Georges Bank. During this meander–WCR interaction, the 20°C isotherm along the northern boundary of the WCR moved 44 km north in 5.25 days (≈ 10 cm s^{-1} northward, compared with the mean translation speed of 6 cm s^{-1} southwestward). As it approached the southern flank, the WCR entrained shelf water seaward at its northeast periphery (Fig. 2a). By May 12, SSW extended from the Scotian Shelf, across the Northeast Channel (NEC), and southwest along the shelfbreak to the northeast periphery of the WCR (Fig. 2a). At that time, the Gulf Stream meander was separating from the WCR.

By May 18 (Fig. 2b), separation of the meander from the WCR was complete. SSW still extended to the filament of shelf water entrained around the WCR. Fluctuating in strength, WCR entrainment continued such that by May 28 (Fig. 2c), entrained shelf water encircled most of WCR periphery. Between May 18 and 28, the WCR moved southwest and ≈ 25 km further seaward of the shelfbreak (cf. Fig. 2b, c). On May 28, SST < 9°C extended across NEC and over a large region of the southern flank between the shelfbreak and the 60-m isobath (Fig. 2c). Along the shelfbreak, this relatively cold water extended beyond the northeast periphery of the WCR, to about 68.4°W, 40.4°N.

SST distributions on May 28 suggest not only southwestward flow of SSW along the southern flank, but also northeastward flow from Great South Channel (GSC). The 9 and 9.5°C isotherms extended northeastward from GSC, along approximately the 60-m isobath (Fig. 2c). This apparent flow pattern met the temperature signature of SSW immediately inshore (on-bank) of the entrained filament of shelf water at the northeast periphery of the WCR (9 and 9.5°C isotherms near 67.6°W, 40.9°N). These SST patterns suggest that horizontal convergence of water masses developed along the southern flank in response to WCR entrainment of shelf water from the southern flank.

The presence and influence of Scotian Shelf water indicated by SST was supported by in situ observation. Salinity < 32 psu, defining SSW during May (Bisagni et al., 1996), extended over northeastern Georges Bank and along the southern flank shelfbreak to ≈ 41°N (Fig. 3). The spatial pattern of lowest salinity suggests flow from the north onto northeastern Georges Bank (note that continuous underway salinity measurement extended north of the domain shown). Over the central southern flank, where surface salinity was > 32, SSW influence was evident subsurface. Average temperature in the layer 20–30 m showed a distinct minimum over hundreds of km^2 (identified as $T_L < 6.2$°C in Fig. 3). On-bank flow was observed near the eastern extremity of this temperature minimum. The vectors in Fig. 3 show average subtidal velocity in the layer 14–26 m (calculated from ADCP total velocity, May 21–23). At the shelfbreak near 66.5°W, 41.2°N, flow was directed west–southwest, on-bank and parallel to the $T_L < 6.2$°C contour near the shelfbreak. Surface temperature observed in situ (not shown) was coldest at this location of onshore flow and over northeastern Georges Bank, i.e. the two locations where SSW apparently flowed onto the bank. Between ≈ 41 and 41.4°N, the 100-m isobath has a local maximum N–S orientation (Figs. 2c and 3). Subsurface temperature and velocity observed between May 21 and 24 (Fig. 3) suggest that

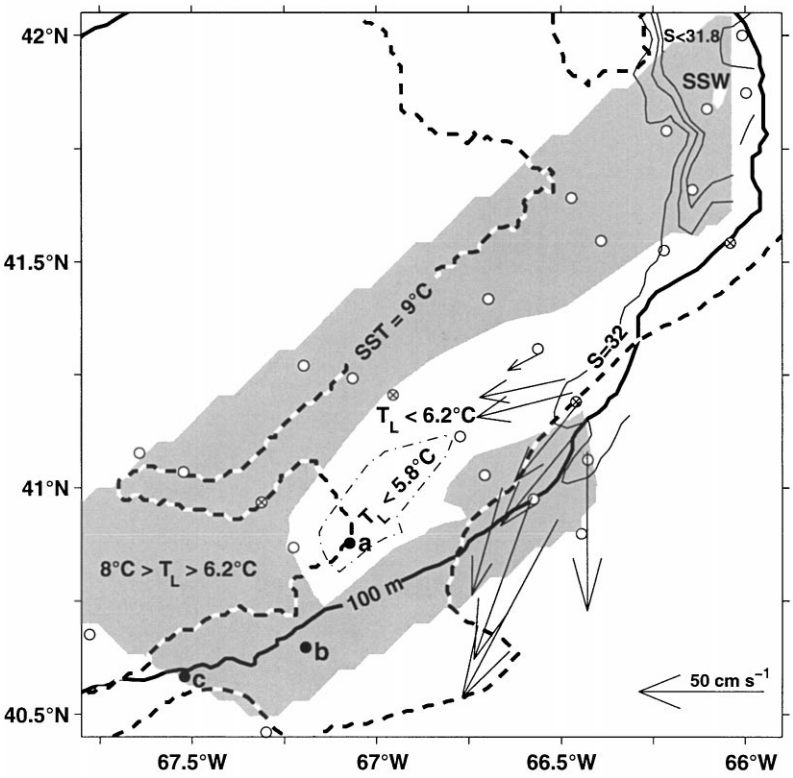

Fig. 3. Hydrographic properties over the southern flank, from CTD survey May 22–24 (domain shown in Fig. 2c). The thick solid contour is the 100-m isobath. T_L (shaded above 6.2°C) is average temperature in the layer 20–30 m. Surface salinity contours (thin solid) less than 32 psu indicate Scotian shelf water (SSW). The dashed contour is the 9°C SST isotherm from 28 May (for reference to Fig. 2c). Labels a–c adjacent the three solid black circles mark the stations for which CTD profiles are shown (Fig. 4). Vectors show average subtidal velocity within the layer 14–26 m.

SSW intrusion onto that region of the bank originated at this local extreme in shelfbreak orientation. The on-bank flow was quite strong (≈ 40 cm s^{-1}), but the strongest flows observed during the survey were seaward of the shelfbreak and were directed toward the WCR entrainment (Figs. 2c and 3).

Over northeastern Georges Bank where surface salinity was < 31.8 and T_L was < 6.2°C (Fig. 3), high chlorophyll concentrations extended throughout SSW in the upper ≈ 20 m. This was the only region of the southern flank where $[NO_2 + NO_3]$ was detectable within the upper 10–20 m. Over other regions of the southern flank, there was a temperature minimum near 30 m underlying a subsurface chlorophyll maximum. To illustrate this water column structure, we present CTD profiles from 3 stations (Fig. 4; locations shown in Fig. 3). These profiles are shown because they were within the region where enhanced chlorophyll was observed by the OCTS (presented in the next section). The temperature minimum near 30 m is interpreted as the depth at which SSW was least diluted by mixing at the time of sampling. Although a temperature minimum was evident near 30 m at all three stations, it was more distinct at the stations seaward of the 100-m isobath

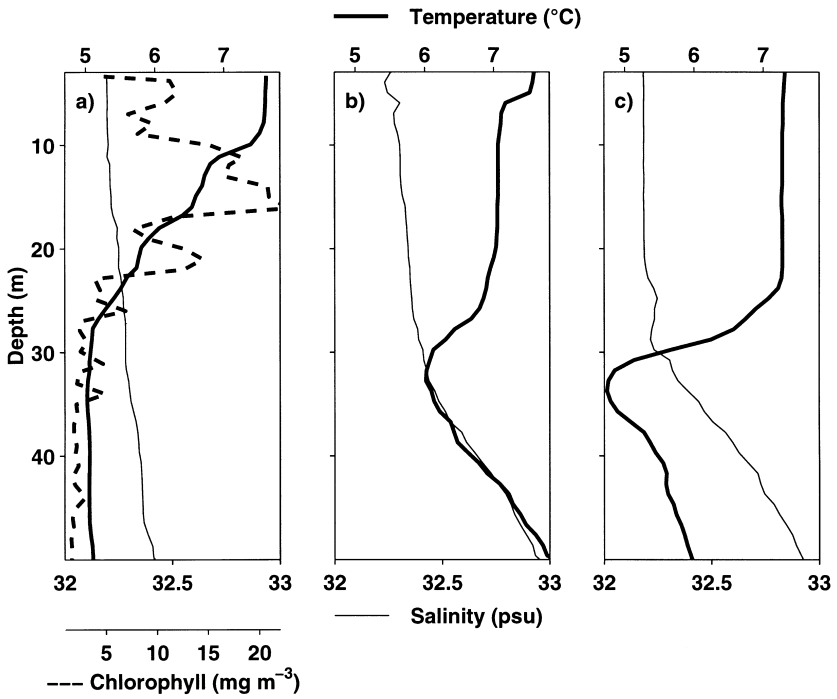

Fig. 4. CTD profiles from the stations labeled a–c in Fig. 3. Only (a) had fluorometry.

(Fig. 4b, c) than at the station over the southern flank (Fig. 4a). At this station, a pronounced subsurface chlorophyll maximum was observed (Fig. 4a) in coincidence with the coldest 20–30 m layer temperature (Fig. 3; $T_L < 5.8°C$). This is consistent with mixing of cold, nutrient rich subsurface SSW above 30 m. Similar water-column physical–biological structure as that shown in Fig. 4a was observed at other stations on the bank. The 4 stations marked by x in Fig. 3 show where this structure was evident (based on limited available CTD fluorometry). All of these stations were where in situ or satellite observations indicated presence of the SSW intrusion. This physical–biological structure was also evident at the shelfbreak further southwest, near Great South Channel. At other stations, SSW properties were pronounced subsurface more in salinity than in temperature. SSW influence extended along the entire southern flank shelfbreak during late May.

3.2. *Surface chlorophyll and temperature observed by satellite*

On May 28, OCTS-Chl exhibited biological structure clearly related to the WCR entrainment of shelf water. The filament of cold shelf water encircling the WCR (Fig. 2c) had much higher chlorophyll concentrations than adjacent WCR and slope water (Fig. 5a). A band of pigment enhancement extended more than 100 km along the southern flank shelfbreak (100-m isobath), in coincidence with the coldest SST ($< 9°C$). When sampled 7 days earlier, this region of the shelfbreak with enhanced chlorophyll showed the presence of the SSW intrusion with a temperature minimum near 30 m (Fig. 4b, c; station locations shown in Fig. 5a). The coldest SST and

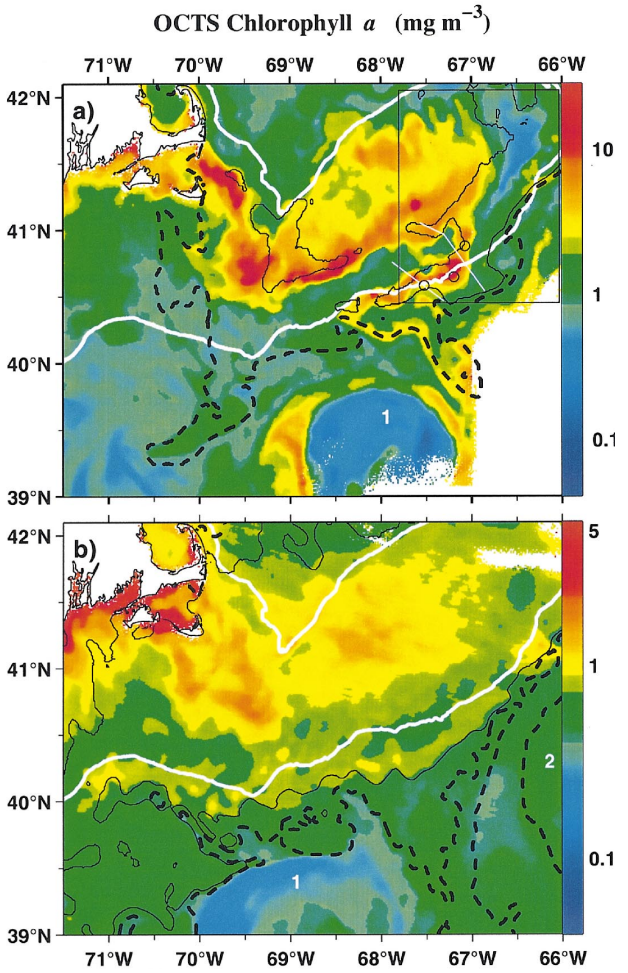

Fig. 5. OCTS chlorophyll images from (a) May 28 and (b) June 11, 1997. Black contours overlaid on each image are same-day SST isotherms. These are (thin solid contour, thick dashed contour): (a) 9 and 11°C; (b) 14 and 17°C (cf. Figs. 5a and 2c for more detail of May 28). The white contour is the 100-m isobath; white numbers identify 2 WCRs. In (a), the box shows the domain of hydrographic observations presented in Fig. 3, circles mark the locations of the three stations for which CTD profiles are shown (Figs. 2–4), and white lines crossing the 100-m isobath show the locations of two transects from the GLOBEC survey (Figs. 7 and 8).

enhanced chlorophyll at the shelfbreak extended only to where the 11°C isotherm and OCTS-Chl indicated seaward flow (≈ 68.5°W, 40.3°N). The enhanced chlorophyll was only evident where maximum offshore displacement of shelf water occurred N-NE of the WCR (Fig. 5a).

A band of high OCTS-Chl also extended southwest–northeast along the 60-m isobath (between ≈ 69°W, 40.5°N and 67°W, 41.4°N). It developed where SSW from the northeast and waters of GSC from the southwest were apparently converging along the 60-m isobath (9°C isotherm in Fig. 5a; as described for Fig. 2c in Section 3.1). The highest chlorophyll within this band was where water from GSC apparently extended northeastward along the 60-m isobath, and this was

the only region where this band of high chlorophyll was evident during the GLOBEC survey (west of 68°W).

Between the two bands of high OCTS-Chl along the 60- and 100-m isobaths, two filaments of enhanced chlorophyll extended across isobaths. One filament was oriented N–S along $\approx 67.1°$W, and the other was oriented NW–SE and centered near 67.6°W, 40.8°N (between the two transect lines in Fig. 5a). These two filaments were inshore of the location where the coldest water ($< 9°$C in Fig. 5a) extended furthest offshore. The two filaments converged to meet at the shelfbreak where OCTS-Chl was highest ($\approx 67.2°$W, 40.7°N). Where the larger of the two filaments developed, in situ properties were sampled 7 days before the OCTS image (northernmost station in Fig. 5a). At this station, the coldest water within the layer 20–30 m had been observed (Fig. 3; $T_L < 5.8°$C) in coincidence with a subsurface chlorophyll maximum (Fig. 4a).

OCTS coverage of the southern flank (not obscured by clouds) nearest May 28 occurred on May 16 and June 11. The biological structure evident on May 28 (Fig. 5a) was not evident on May 16. However, on June 11, there was a local maximum in OCTS-Chl slightly offshore of and parallel to the 100-m isobath south of Georges Bank and Cape Cod, centered north of the WCR (Fig. 5b). Its spatial extent was greater than that observed on May 28, but its magnitude was lower (absolute and relative to background). Near the northeast periphery of the WCR (isotherms between 67 and 68°W in Fig. 5b), the along-shelf extent of isotherm displacement and its position relative to the WCR on June 11 were similar to that observed on May 28 (Fig. 5a). Additionally, isotherms near the NW periphery of the WCR suggest water mass exchange. SST $< 14°$C south of 40°N and west of 69.5°W formed an apex along the ring periphery near 69.5°W, 39.5°N, consistent with entrainment by the anticyclonic circulation of the WCR. Indicating onshore counter-flow of relatively warm WCR or slope water, the 14 and 17°C isotherms extended toward the region of enhanced shelfbreak chlorophyll (north of 39.5°N, between 69.5 and 71.2°W).

Waves of the shelf-slope front, coincident with the enhanced chlorophyll west of $\approx 67.5°$W (14°C isotherm in Fig. 5b), were also evident. The waves had an average wavelength of ≈ 30 km and amplitude of ≈ 15 km. They propagated west at ≈ 12 km day^{-1} (estimated from a sequence of SST imagery), and water mixed across the front as they broke. The 14°C isotherm defines the approximate seaward limit of the waves, and their breaking was pronounced along their shoreward limit, closer to the 100-m isobath.

3.3. Processes associated with enhanced chlorophyll

$[NO_2 + NO_3]$ measured during the late May GLOBEC survey showed nutrient depletion of the upper 10–20 m of southern flank shelf waters, except where SSW occupied the upper ≈ 20 m over northeastern Georges Bank. Satellite observations showed that the enhanced chlorophyll along the shelfbreak during late May and mid-June was not present during mid-May. Because satellite-derived chlorophyll is representative of only the upper optical depth (upper ≈ 10 m at most), local enhancement of near-surface chlorophyll at the shelfbreak must have occurred during late May and June. Such localized enhancement of chlorophyll could occur by enhanced growth due to nutrient input, or by shoaling of subsurface chlorophyll. These causative factors would require vertical flux, either by upwelling or vertical mixing. Using the combined satellite and in situ observations, we consider processes coincident with the local chlorophyll enhancement along the shelfbreak during late May and mid-June 1997.

Before considering evidence for processes, we introduce them conceptually (Fig. 6). In this schematic representation, solid lines indicate observed patterns, and dashed lines indicate dynamics inferred from observations. Each process is represented in the plane appropriate to the observations. Process 1 is upwelling resulting from divergent flow. Process 2 is turbulent vertical mixing driven by vertical shear in horizontal velocity. Estimated gradient Richardson numbers were the relevant measure for this process (see methods). The line from this process representation into the cross-shelf plane indicates that it was important near the shelfbreak. Although along-shelf jets were pronounced, strong vertical shear was evident in both velocity components used to define Ri (Eq. (1)). Process 3 is vertical mixing forced by breaking frontal waves. Examination of this process is unique in that no in situ observations were available at the time the waves were observed by satellite. The vertical scale of mixing by this process is proportional to the slope of the front (cross-shelf plane).

During the late May GLOBEC survey of the southern flank, two transects were made across the enhanced chlorophyll at the shelfbreak. These transects were made 7 and 6 days, respectively, prior to the OCTS observations of May 28 (transect locations shown in Fig. 5a; transect 1 southwest of transect 2). Because in situ observations preceded satellite observations by 1 week, we do not expect the two sources of observations to match exactly. Owing to advection, mixing, and biological processes, significant changes in hydrographic and biological distributions would have occurred during the period between in situ and satellite observation.

Transect 1: Along transect 1, two chlorophyll maxima were observed in situ near the shelfbreak (Fig. 7a). One was centered ≈ 5 km south of the shelfbreak, and the other was centered ≈ 18 km north of the shelfbreak. Each chlorophyll maximum coincided with a local temperature minimum (Fig. 7b), and a local maximum of subtidal along-shelf velocity between ≈ 30 and 40 m (Fig. 7d).

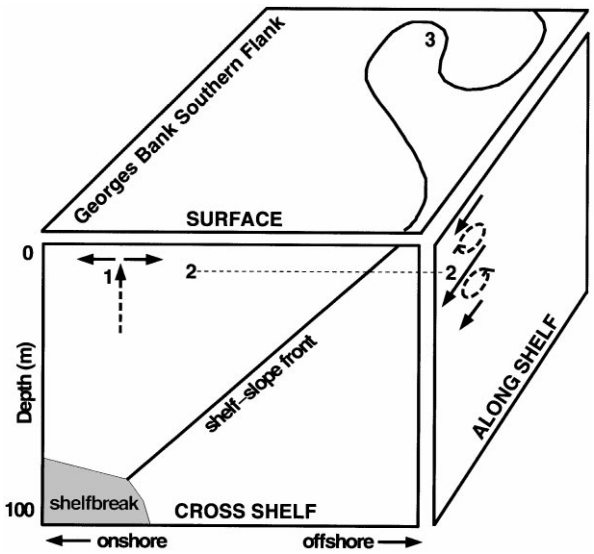

Fig. 6. Schematic of processes evident in association with the enhanced shelfbreak chlorophyll south of Georges Bank during late spring–early summer 1997. See text for explanation.

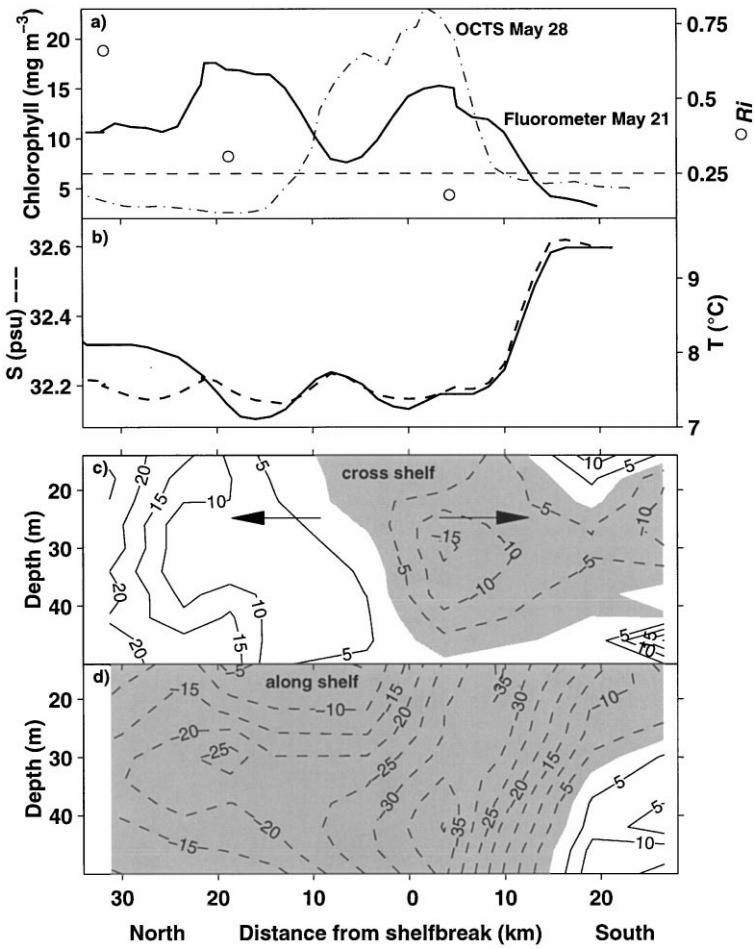

Fig. 7. Transect 1, the more southwestern transect shown in Fig. 5a. (a) Surface fluorometric chlorophyll (solid line), OCTS-Chl (dash-dot line), and Ri (median Ri in the layer 9–20 m, circles); (b) surface salinity and temperature; (c) cross-shelf subtidal velocity; (d) along-shelf subtidal velocity. All observations are from May 21 except OCTS-Chl.

They were centered over divergence of subtidal cross-shelf flow (Fig. 7c; process 1 in Fig. 6). Ri was lower within the two chlorophyll maxima than at the station furthest north (Fig. 7a). Ri was lowest (< 0.25) in coincidence with the strongest along-shelf jet and offshore flow at the shelfbreak (Fig. 7a, c, d; 5 km south of the shelfbreak), where the SSW intrusion was observed in situ (Fig. 4c), and where OCTS-Chl was highest 7 days later (Fig. 7a).

Transect 2: Across the northeast extremity of the shelfbreak chlorophyll enhancement, the chlorophyll maximum was broader than it was to the southwest (Fig. 5a). It narrowed from ≈ 50 km on May 22 to ≈ 20 km on May 28 (Fig. 8a). The band of enhanced chlorophyll along the 60-m isobath observed by OCTS on May 28 was not evident when the region was sampled on May 22 (Fig. 8a, 40 km north of the shelfbreak). As along transect 1, the shelfbreak chlorophyll maximum coincided with divergent cross-shelf flow (Fig. 8c) and maximum southwestward along-shelf velocity (Fig. 8d). The transition into the chlorophyll maximum near 35 km north of the shelfbreak

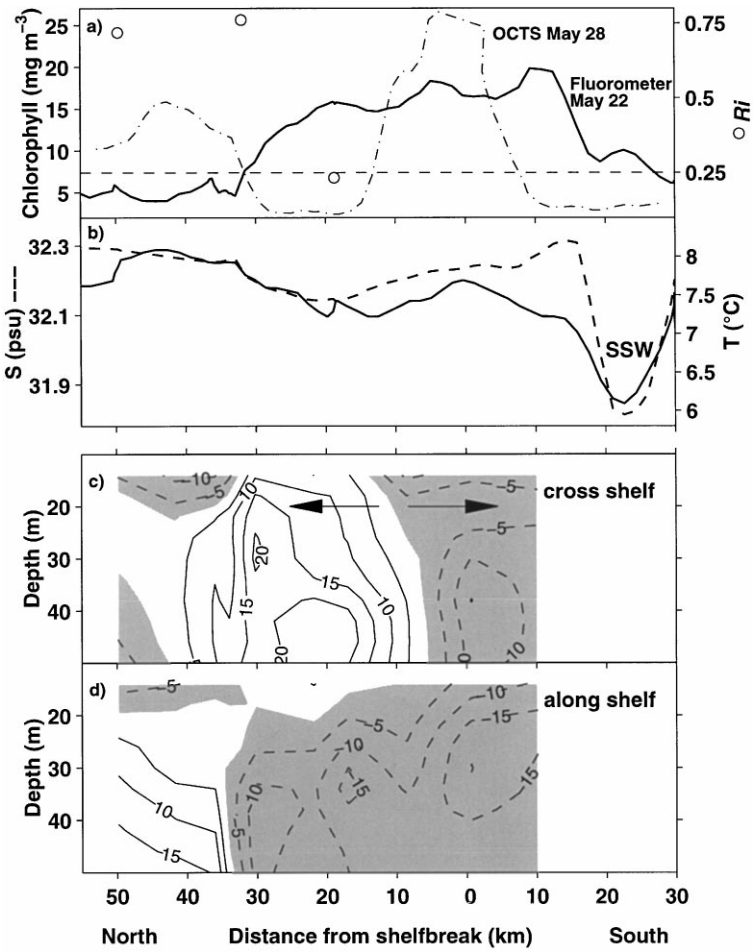

Fig. 8. Transect 2, the more northeastern transect shown in Fig. 5a. (a) Surface fluorometric chlorophyll (solid line), OCTS-Chl (dash-dot line), and Ri (median Ri in the layer 9–20 m, circles); (b) surface salinity and temperature; SSW label identifies Scotian shelf water properties; (c) cross-shelf subtidal velocity; (d) along-shelf subtidal velocity. The seaward limit of velocity observations is defined by the limit of ADCP bottom tracking. All observations are from May 22 except OCTS-Chl.

(Fig. 8a) coincided with decreases in surface temperature and salinity (Fig. 8b). This is consistent with influence of the subsurface intrusion (Fig. 4) on near-surface temperature and salinity. Ri was below critical within the shelfbreak chlorophyll maximum, and above critical further north. Ri could not be calculated within the southern half of the broad chlorophyll maximum due to a lack of CTD observations. SSW was also observed near the surface along this transect, $\approx$ 15–30 km south of the shelfbreak (Fig. 8b). This region of SSW was not sampled by CTD, so its vertical structure could not be defined (note also that it is not shown in Fig. 3). Near-surface fluorometric chlorophyll was relatively high within the SSW (Fig. 8a).

The transects showed a relationship between surface chlorophyll and Ri (representing the potential for turbulent vertical mixing in the upper water column). During the survey of the

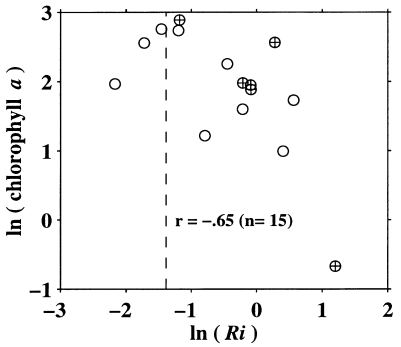

Fig. 9. Median Ri in the layer 9–20 m, representing the potential for turbulent vertical mixing in the upper water column, versus surface fluorometric chlorophyll for stations on the bank and within 20 km of the shelfbreak between 66 and 68°W. + symbols mark stations where CTD profiles were from the *Mark V* instrument (see methods).

southern flank between May 21 and 24, there was also a significant ($p < 0.005$) inverse correlation between surface chlorophyll concentrations and Ri (Fig. 9). Considering the southernmost 20 km of the southern flank between 66 and 68°W (domain based on in situ sampling), a positive gradient in chlorophyll from northeast to southwest coincided with a negative gradient in Ri. The spatial distribution of Ri was controlled by shear: correlation between Ri and the shear term (denominator of Eq. (1)) was -0.85 (significant at $p < 0.005$); correlation between Ri and the stratification term (numerator of Eq. (1)) was near zero.

During mid-June, shelf water entrainment by the WCR was still evident in SST (Section 3.2). Thus the same processes evident during late May (divergence of cross-shelf flow, along-shelf jets and associated shear-driven turbulent vertical mixing) may have been important at that time. In addition, breaking frontal waves were observed in coincidence with the enhanced shelfbreak chlorophyll west of $\approx 67.5°$W. Considering a wave amplitude of ≈ 15 km and a mean frontal slope of $\approx 1–2 \times 10^{-3}$, the vertical scale of mixing across the front when the waves break would be $\approx$ 15–30 m. Thus their breaking could have forced significant vertical mixing at the front.

4. Discussion

The continental shelf ecosystem of the northeast US is among the most productive in the global ocean (O'Reilly and Bush, 1984; O'Reilly et al., 1987; Walsh et al., 1987). Due to seasonal variation of density stratification in this ecosystem, the vertical distributions of phytoplankton primary production and biomass cycle seasonally (Malone et al., 1983; O'Reilly et al., 1987; O'Reilly and Zetelin, 1998). Winter conditions are one extreme, when low incident irradiance and deep mixing impose light limitation on primary production. As the mixed layer shoals with the development of stratification, increasing light exposure within the mixed layer promotes the winter–spring bloom (Sverdrup, 1953; Smetacek and Passow, 1990). After near-surface nutrients are exhausted during spring, intensifying stratification progressively inhibits the vertical mixing that can replenish nutrients above the seasonal thermocline. The upper 20–30 m of regional shelf waters become nutrient depleted by approximately May (Ketchum et al., 1958; Walsh et al., 1987). This leads to the

other extreme of summer, when phytoplankton growth remains nutrient limited above the thermocline, and a subsurface chlorophyll maximum develops within the thermocline.

By influencing water column stability and vertical flow, the shelfbreak front influences phytoplankton processes at the shelfbreak throughout the year. During winter–spring, phytoplankton bloom relatively early at the shelfbreak where shoaling of the mixed layer by the front locally increases light exposure (Marra et al., 1982; Malone et al., 1983). During summer, phytoplankton production is enhanced at the shelfbreak when nutrient rich shelf water transported offshore is upwelled along frontal isopycnals (Malone et al., 1983; Marra et al., 1990). Upwelling of ≈ 9 m day^{-1} can develop on the inshore side of the front during summer due to convergence in the bottom boundary layer at the shelfbreak (Barth et al., 1998). Summer stratification restricts enhanced shelfbreak chlorophyll below the depth to which satellite remote sensing can detect. However, during the transitional period between the spring bloom and the strongly stratified conditions of summer, enhancement of chlorophyll in near-surface waters, visible to satellite remote sensing, develops annually along the shelfbreak front of the MAB and Georges Bank (Ryan et al., 1999a). This annual ecological feature can persist well into the period of near-surface nutrient limitation, thus local nutrient and/or pigment enrichment at the front is fundamental to its development.

During late spring of 1997, two occurrences of enhanced chlorophyll along the northeast US continental shelfbreak were observed by the OCTS. The first was during early May, when enhanced chlorophyll developed along $>$ 200 km of the MAB shelfbreak. Its dynamical basis was upwelling along frontal isopycnals as shelf water was transported seaward by the circulation of shelfbreak frontal meanders (Ryan et al., 1999b). Definition of this process was possible only with high-resolution SeaSoar observations across the shelfbreak front. The second occurrence was during late May, when enhanced chlorophyll developed along $>$ 100 km of the Georges Bank shelfbreak in association with WCR entrainment of shelf water (illustrated herein). This biological structure was not evident in satellite ocean color during mid-May, so its development during late May implies local enhancement of phytoplankton biomass in near-surface waters. This could occur by enhanced growth in response to upwelled nutrients and/or shoaling of subsurface pigments.

The combined satellite and GLOBEC survey observations permitted definition of processes important to chlorophyll distributions along the southern flank during late May. Although the cross-shelf dimension of the enhanced shelfbreak chlorophyll changed during the 6–7 day period between in situ and satellite observation, the local enhancement remained a distinct feature during this period. It developed where shelf waters were displaced furthest seaward N–NE of the WCR, supporting the underlying importance of the WCR entrainment to its development and to the processes observed in coincidence with its development.

Both in situ and satellite observations showed that the enhanced chlorophyll coincided with locally cold surface water. SSW was the coldest water mass sampled, and over much of the bank it was pronounced as a subsurface temperature minimum near 30-m depth. Satellite SST 6–7 days after this in situ sampling indicated that SSW had influenced surface temperatures over a large region of the southern flank, but the coldest SST was along the shelfbreak. Across both transects, the enhanced shelfbreak chlorophyll coincided with divergent cross-shelf flow (consistent with upwelling) and along-shelf jets and associated vertical shear (consistent with turbulent vertical mixing). The role of turbulent vertical mixing was supported. Ri was below critical within the enhanced shelfbreak chlorophyll along both transects, and surface chlorophyll along the southern flank was significantly, inversely correlated with Ri. The distribution of Ri was controlled by shear;

this supports the role of the observed along-shelf jets and their vertical shear. The presence of along-shelf jets and divergent cross-shelf flow at locations separated by 40 km supports their combined role in the development of cold, pigment-rich, near-surface waters at the shelfbreak.

The scale of the frontal waves observed during mid-June is consistent with that of waves generated by horizontal shear between the shelfbreak frontal jet (Aikman III et al., 1988; Gawarkiewicz et al., 1996) and a WCR. Shear-generated frontal waves occur in this region during late spring, they extend to ≈ 100 m, and they are believed to break and mix water across the front (Ramp et al., 1983; Ramp, 1986). However, the waves observed in this study propagated in the opposite direction as these previously described frontal waves. Thus the dynamical basis for the frontal waves described here is unknown.

Scotian Shelf water strongly influenced Georges Bank hydrography during May 1997. SSW is known to flow onto Georges Bank and contribute to the shelf water mass (Hopkins and Garfield III, 1981; Bisagni et al., 1996). The distribution of SSW described here from salinity is similar to that observed in 1992 and that defined from climatology (Bisagni et al., 1996). A definitive property of SSW ($S < 32$ psu) was observed near-surface only over northeastern Georges Bank and along the southern flank shelfbreak. However, satellite and in situ temperature distributions defined more widespread SSW influence over the southern flank between the 60-m isobath and the shelfbreak front, consistent with mixing of the subsurface SSW intrusion with resident shelf water. The importance of Scotian Shelf water to hydrographic conditions over the southern flank during this period was also supported by T/S anomaly fields (Mountain et al., 1997). Surface and bottom T/S exhibited significant negative anomalies along most of the southern flank during the late May survey. $[NO_2 + NO_3]$ were detectable within the upper 10–20 m only within the SSW over northeast Georges Bank. This water mass was relatively nutrient rich, and as it intruded and mixed with resident shelf waters along the southern flank, it influenced hydrographic, nutrient, and biological distributions.

WCR interactions with shelf water masses have important implications for fisheries oceanography and shelf carbon budgets. Existing evidence supports the conclusion that shelf water entrained by WCRs derives from a relatively narrow band along the shelf water side of the shelfbreak front, extending both ahead of and behind a WCR (Ramp, 1986; Schlitz, 1999). The band of enhanced OCTS-Chl along the Georges Bank shelfbreak during late May 1997, when WCR entrainment was extreme, extended both ahead of and behind the WCR. Thus the spatial distribution of this biological enhancement is consistent with definition of entrainment source water from analyses of hydrographic properties. However, hydrographic properties during late May indicated widespread changes in water mass distributions on and around Georges Bank. Source water for WCR entrainment would depend on numerous variables, including proximity of the WCR to the shelfbreak, and intensity and duration of entrainment. Analyses of more WCR entrainment occurrences is required to define variation in source waters, and influence on larval recruitment and carbon flux. Understanding WCR influence on shelf ecology requires the combined strengths of satellite remote sensing and high-resolution in situ observation.

Acknowledgements

This research was supported by NASA grant NAG5-6645. We thank the National Space Development Agency of Japan and W. Gregg at NASA Goddard Space Flight Center (GSFC) for

the OCTS imagery. OCTS processing software was provided by the SeaDAS Development Group at GSFC. AVHRR imagery was provided by P. Cornillon and D. Holloway. AVHRR satellite data processing software was developed by R. Evans, O. Brown, J. Brown, and A. Li of the University of Miami. Hydrographic data and alongtrack T/S were provided by D. Mountain, M. Taylor, and J. Manning. G. Strout provided calibration information for the thermosalinograph, and P. Garrahan provided the regression coefficients for calibration of the CTD fluorometer. The code for processing broadband ADCP data was written by H. Seim, and C. Flagg provided the MATLAB code for the Georges Bank tidal analysis. US GLOBEC contribution 138.

References

Aikman III, F., Ou, H.W., Houghton, R.W., 1988. Current variability across the New England continental shelf-break and slope. Continental Shelf Research 8, 625–651.

Barth, J.A., Bogucki, D., Pierce, S.D., Kosro, P.M., 1998. Secondary circulation associated with a shelfbreak front. Geophysical Research Letters 25, 2761–2764.

Bisagni, J.J., Beardsley, R.C., Ruhsam, C.M., Manning, J.P., Williams, W.J., 1996. Historical and recent evidence of Scotian Shelf water on southern Georges Bank. Deep-Sea Research Part II 43, 1439–1471.

Brown, O.B., Cornillon, P.C., Emmerson, S.R., Carle, H.M., 1986. Gulf Stream warm-core rings: a statistical study of their behavior. Deep-Sea Research Part I 33, 1459–1473.

Brown, W.S., Moody, J.A., 1987. Tides. In: Backus, R.H., Bourne, D.W. (Eds.), Georges Bank. MIT Press, Cambridge, MA, pp. 100–107.

Candela, J., Beardsley, R.C., Limeburner, R., 1992. Separation of tidal and subtidal currents in ship-mounted acoustic Doppler current profiler observations. Journal of Geophysical Research 97, 769–788.

Churchill, J.H., Levine, E.R., Connors, D.N., Cornillon, P.C., 1993. Mixing of shelf, slope and Gulf Stream water over the continental slope of the Middle Atlantic Bight. Deep-Sea Research Part I 40, 1063–1085.

Churchill, J.H., Cornillon, P.C., Milkowski, G.W., 1986. A cyclonic eddy and shelf-slope water exchange associated with a Gulf Stream warm-core ring. Journal of Geophysical Research 91, 9615–9623.

Evans, R.H., Baker, K.S., Brown, O.B., Smith, R.S., 1985. Chronology of warm-core ring 82B. Journal of Geophysical Research 90, 8803–8811.

Flagg, C.N., 1987. Hydrographic structure and variability. In: Backus, R.H., Bourne, D.W. (Eds.), Georges Bank. MIT Press, Cambridge, MA, pp. 108–124.

Fofonoff, N.P., Millard, R.C., 1983. Algorithms for calculation of fundamental properties of seawater. UNESCO Technical Papers in Marine Science, No. 44, 53 pp.

Garcia-Moliner, G., Yoder, J.A., 1994. Variability in pigment concentrations in warm-core rings as determined by coastal zone color scanner satellite imagery from the Mid-Atlantic Bight. Journal of Geophysical Research 99, 14,277–14,290.

Garfield, N., Evans, D.L., 1987. Shelf water entrainment by Gulf Stream warm-core rings. Journal of Geophysical Research 92, 13,003–13,012.

Gawarkiewicz, G., Ferdelman, T.G., Church, T.M., Luther III, G.W., 1996. Shelfbreak frontal structure on the continental shelf north of Cape Hatteras. Continental Shelf Research 16, 1751–1773.

Gilman, C.S., 1988. A study of the Gulf Stream downstream of Cape Hatteras, 1975–1986. M. S. Thesis, University of Rhode Island.

Gordon, H.R., Clark, D.K., Brown, J.W., Brown, O.B., Evans, R.W., Broenkow, W.W., 1983. Phytoplankton pigment concentrations in the Middle Atlantic Bight: comparison of ship determinations and CZCS estimates. Applied Optics 22, 20–36.

Haliwell, G.R., Mooers, C.N.K., 1979. The space-time structure and variability of the shelf water-slope water and Gulf Stream surface temperature fronts and associated warm-core eddies. Journal of Geophysical Research 84, 7707–7725.

Hopkins, T.S., Garfield III, N., 1981. Physical origins of Georges Bank water. Journal of Marine Research 39, 465–500.

Joyce, T.M., 1984. Velocity and hydrographic structure of a Gulf Stream warm-core ring. Journal of Physical Oceanography 14, 936–947.

Kennelly, M., Evans, R.H., Joyce, T.M., 1985. Small-scale cyclones on the periphery of a Gulf Stream warm-core ring. Journal of Geophysical Research 90, 8845–8857.

Ketchum, B.H., Vaccaro, R.F., Corwin, N., 1958. The annual cycle of phosphorous and nitrogen in New England coastal waters. Journal of Marine Research 17, 282–301.

Malone, T.C., Hopkins, T.S., Falkowski, P.G., Whitledge, T.E., 1983. Production and transport of phytoplankton biomass over the continental shelf of the New York Bight. Continental Shelf Research 1, 305–337.

Marra, J., Houghton, R.W., Boardman, D.C., Neale, P.J., 1982. Variability in surface chlorophyll *a* at a shelf-break front. Journal of Marine Research 40, 575–591.

Marra, J., Houghton, R.W., Garside, C., 1990. Phytoplankton growth at the shelf-break front in the Middle Atlantic Bight. Journal of Marine Research 48, 851–868.

McClain, C.R., Fraser, R.S., McLean, J.T., Darzi, M., Firestone, J.K., Patt, F.S. et al., 1994. In: Case Studies for SeaWiFS Calibration and Validation, Part 2. NASA Technical Memo 104566, Vol. 19, Hooker, S.B., Firestone, E.R., Acker, J.G. (Eds.), NASA/Goddard Space Flight Center, Greenbelt, MD.

Moody, J.A., Butman, B., Beardsley, R.C., Brown, W.S., Danifuku, P., Irish, J.D. et al., 1984. Atlas of Tidal Elevation and Current Observations on the Northeast American Continental Shelf and Slope. U.S. Geological Survey Bulletin, Vol. 1611, U.S. Government Printing Office.

Morgan, P.P., 1992. CSIRO Oceanographic Toolbox for MATLAB. Online, ftp://aqueous.ml.csiro/pub/morgan/seawater.

Mountain, D., Taylor, M., Chute, A., Sibunka, J., Weiner, A., Crain, J. et al., 1997. Cruise Report: R/V ALBATROSS IV, Cruise 9705 to Georges Bank, 19–27 May 1997. NOAA, Woods Hole, MA.

Nelson, D.M., McCarthy, J.J., Joyce, T.M., Ducklow, H.W., 1989. Enhanced near-surface nutrient availability and new production resulting from frictional decay of a Gulf Stream warm-core ring. Deep-Sea Research Part I 36, 705–714.

O'Reilly, J.E., Zetelin, C., 1998. Seasonal, horizontal, and vertical distribution of phytoplankton chlorophyll a in the northeast U.S. continental shelf ecosystem. NOAA Technical Report NMFS 139, U. S. Department of Commerce, Seattle, 120 pp.

O'Reilly, J.E., Zetelin, C., Bush, D.A., 1987. Primary production. In: Backus, R.H., Bourne, D.W. (Eds.), Georges Bank. MIT Press, Cambridge, MA, pp. 221–233.

O'Reilly, J.E., Bush, D.A., 1984. Phytoplankton primary production on the northwestern Atlantic shelf. Rapports et Proces verbaux des Reunions Conseil International pour l'Exploration de la Mer, Vol. 183, pp. 255–268.

Pond, S., Pickard, G.L., 1983. Introductory Dynamical Oceanography. Pergamon, New York.

Ramp, S.R., Beardsley, R.C., Legeckis, R., 1983. An observation of frontal wave development on a shelf-slope/warm core ring front near the shelfbreak south of New England. Journal of Physical Oceanography 13, 907–912.

Ramp, S.R., 1986. The interaction of warm core rings with the shelf water and shelf-slope front south of New England. Ph.D. Thesis, University of Rhode Island.

Richardson, P.L., 1983. Gulf Stream rings. In: Robinson, A.R. (Ed.), Eddies in Marine Science. Springer, Berlin, pp. 19–64.

Ryan, J.P., Yoder, J.A., Cornillon, P.C., 1999a. Enhanced chlorophyll at the shelfbreak of the Mid-Atlantic Bight and Georges Bank during the spring transition. Limnology and Oceanography 44, 1–11.

Ryan, J.P., Yoder, J.A., Barth, J.A., Cornillon, P.C., 1999b. Chlorophyll enhancement and mixing associated with meanders of the shelfbreak front in the Mid-Atlantic Bight. Journal of Geophysical Research 104, 23 479–23 493.

Saitoh, S., Miyoi, T., Kishino, M., 1997. Development of bio-optical algorithm for ocean color remote sensing in the sub-arctic North Pacific ocean. SPIE 2963, 766–771.

Saunders, P.M., 1971. Anticyclonic eddies formed from shoreward meanders of the Gulf Stream. Deep-Sea Research Part I 18, 1207–1219.

Schlitz, R.J., 1999. The interaction of shelf water with warm-core rings. NOAA Technical Report, U. S. Department of Commerce.

Smetacek, V., Passow, U., 1990. Spring bloom initiation and Sverdrup's critical-depth model. Limnology and Oceanography 35, 228–234.

Smith, R.C., Baker, K.S., 1985. Spatial and temporal patterns in pigment biomass in Gulf Stream warm-core ring 82B and its environs. Journal of Geophysical Research 90, 8859–8870.

Sverdrup, H.U., 1953. On conditions for the vernal blooming of phytoplankton. Journal du Conseil International pour l'Exploration de la Mer 18, 287–295.

Walsh, J.J., et al., 1987. Nitrogen cycling on Georges Bank and the New York shelf: a comparison between well-mixed and seasonally-stratified waters. In: Backus, R.H., Bourne, D.W. (Eds.), Georges Bank. MIT Press, Cambridge, MA, pp. 234–246.

Wright, W.R., 1976. The limits of shelf water south of Cape Cod. Journal of Marine Research 34, 1–14.

Wright, W.R., Parker, C.E., 1976. A volumetric temperature/salinity census for the Middle Atlantic Bight. Limnology and Oceanography 21, 563–571.

Yentsch, C.S., Phinney, D.A., 1985. Rotary motions and convection as a means of regulating primary production in warm core rings. Journal of Geophysical Research 90, 3237–3284.